

# Morphological characterization of diamond coatings grown by MWPECVD on hexagonal Boron Nitride

Giorgio S. Senesi<sup>1\*</sup>, Grazia Cicala<sup>2</sup>

<sup>1,2</sup>Istituto di Nanotecnologia, (NANOTEC), CNR, Via Amendola 122/D, 70126, Bari, Italy

**Abstract**— *A relevant and still unsolved issue in the characterization of diamond coatings deposited on ceramic materials such as hexagonal boron nitride (h-BN) is to enhance the resistance of the substrate to erosion by Kr+ or Xe+ ions generated in the plasma propulsion systems. In this work, diamond films were grown by microwave plasma enhanced chemical vapour deposition on h-BN substrates untreated, for the first time, and pre-treated for short (31-65 min) and long (285-296 min) process times. The morphology of diamond films was analysed by scanning electron microscopy, and atomic force microscopy, and their chemistry and structure by Raman spectroscopy. Microscopy analysis revealed that non-continuous (at short process time) and continuous (at long process time) films were formed, respectively, on both untreated and pre-treated h-BN substrates. In particular, diamond films grown on untreated h-BN substrates exhibited roughness values higher than those of h-BN substrates pre-treated by a conventional ultrasonic method.*

**Keywords:** *Insulators; chemical vapour deposition (CVD); coatings; crystal growth; plasma deposition; atomic force microscopy (AFM); scanning electron microscopy (SEM); Raman spectroscopy; surface properties*

## I. INTRODUCTION

The space exploration program faces enormous challenges as it seeks to achieve significant improvements in safety, cost and speed of missions to the frontiers of space. Plasma propulsion systems have been recognized to be more efficient than chemical thrusters, but substrates in contact with the discharge need to be highly resistant to ion erosion. This fact led to the development of highly efficient electric propulsion thrusters that are currently the only feasible technology in many deep space missions.<sup>1</sup> However, the sputter erosion of the discharge channel walls due to ion impingement is one of the main life-limiting factors of the system. During a normal operation, a small fraction of accelerated ions impacts the interior of the main discharge channel, thus causing its gradual erosion during long operational times (from thousands to tens of thousands of hours).<sup>1</sup>

Materials such as Mo, which shows sputter-resistant surfaces, have been fabricated and used in electric propulsion thrusters to lengthen their life.<sup>2</sup> Further, carbon-based materials have shown an improvement of nearly an order-of-magnitude over Mo in sputter erosion resistance.<sup>3</sup> In particular, among the tested carbon-based materials, diamond films prepared by chemical vapour deposition (CVD) have provided an improvement by a factor of 1.5 over other materials in sputter erosion rate.<sup>4</sup>

Boron Nitride (BN) has also raised a high interest in the area of material sciences and its use as an insulator in space electric propulsion thrusters. This is due to the special bonding features of boron and nitrogen, its chemical inertness at high-temperature and its high thermal conductivity and low dielectric constant.<sup>5-7</sup> BN exists in many different structures, of which two forms, i.e. its only two stable phases, are of particular interest: the cubic allotrope of BN (c-BN), which exhibits an extreme hardness that makes it a promising material for protective and abrasive coatings; and the hexagonal allotrope of BN (h-BN), which shows optimal insulating features. The h-BN has characteristics similar and is iso structural to graphite, i.e. it shows layered sp<sup>2</sup>-bonded structure where each carbon atom is replaced by boron and a nitrogen atom, respectively. For its colour it is also known as “white graphite”<sup>6</sup>. The major differences between h-BN and graphite are the electrical and optical properties, i.e., graphite is an electrical conductor, whereas h-BN is an insulator. Further, h-BN is the only BN phase found in nature and can be easily synthesized and machinable.

Bulk h-BN is widely used in several applications because of its interesting properties, including low density, chemical inertness, stability in air at high temperatures (up to 1000°C), stability to thermal shocks, easy workability as hot-pressed shapes, and excellent electrical insulating features as a ceramic material. Due to these specific properties, h-BN has been used in space electric propulsion thrusters,<sup>1,8</sup> to construct crucibles and molds for melting glass and metals for high-

temperature applications, as a very high thermal conductor,<sup>6,7</sup> as a protective layer on surfaces,<sup>9-16</sup> as a substrate for electronic devices,<sup>17-23</sup> as an additive in engine oils and plastics,<sup>24-27</sup> and as a solid lubricant.<sup>5</sup>

Diamond is well known to feature a high sputter resistance to bombardment by Xe ions, the highest thermal conductivity of all insulators, and the lowest dielectric constant. The limited experimental data available on Xe-ion induced sputter yield suggest that, when comparing various wall material options including diamond, alumina ( $\text{Al}_2\text{O}_3$ ) and BN, the sputter resistance of polycrystalline diamond is 25% better than that of BN.<sup>28</sup> In a preliminary study by Yap et al.,<sup>2</sup> ion erosion of multiwall nanotubes by Kr ions generated by a Hall effect thruster was compared to that of CVD diamond films, c-BN and amorphous-carbon (a-C) films. The CVD diamond films were found to have a resistance to ion erosion higher than that of vertically-aligned multiwall nanotubes.

Most studies on diamond growth on BN used bulk c-BN crystal substrates obtained by high-pressure methods,<sup>29,30</sup> whereas only one study has dealt with diamond growth on h-BN films.<sup>31</sup> The latter authors demonstrated the feasibility of growing high quality polycrystalline continuous diamond films by hot filament CVD onto a pre-treated PECVD h-BN film about 2- $\mu\text{m}$  thick deposited on a Si (100) substrate.

The main objective of the present work was to find a means to avoid the sputtering of h-BN insulator walls of Hall thrusters by growing diamond coatings on untreated, for the first time, and pre-treated h-BN substrates by microwave plasma enhanced chemical vapour deposition (MWPECVD) using  $\text{CH}_4/\text{H}_2$  gas mixtures. The first part of this research was focused on the evaluation of growth of diamond coatings by pyrometric interferometry (PI). In the second part, the morphological characterization of diamond films grown at short (31-65 min) and long (285-296 min) process times was studied by scanning electron microscopy (SEM) and atomic force microscopy (AFM), and the nature of chemical bonding by Raman spectroscopy.

## II. MATERIALS AND METHODS

Pieces of p-Si (20 mm x 10 mm x 0.5 mm) and an h-BN disk (diameter 25 mm, 0.8 mm thick) were used as substrates for diamond deposition. The h-BN samples were polished with fine grit sand paper. The diamond films were obtained by the MWPECVD technique in a homemade cylindrical stainless-steel Astex-type reactor. The double-walled and water-cooled reactor forms a resonant cavity for 2.45 GHz microwaves. A Sairem GMP 20KED/RI1325 microwave generator working in continuous wave (CW) mode was used to transmit the power into the cavity and to generate in its centre a discharge having the shape of a symmetric ball.

TABLE 1

**DEPOSITION TEMPERATURE ( $T_D$ ), PROCESS TIME ( $t_p$ ), DEPOSITION RATE ( $R_D$ ) AND COATING THICKNESS ( $d_{\text{coating}}$ ) MEASURED BY PYROMETRIC INTERFEROMETRY (PI), AND ROOT MEAN SQUARE ROUGHNESS MEASURED ( $R_{\text{RMS}}$ ) BY ATOMIC FORCE MICROSCOPY (AFM) FOR THE FOUR INVESTIGATED DIAMOND FILMS GROWN ON UNTREATED AND PRE-TREATED h-BN SUBSTRATES**

| Samples             | $T_D$<br>[°C] | $t_p$<br>[min] | $R_D$<br>[ $\mu\text{m}/\text{h}$ ] | $d_{\text{coating}}$<br>[nm] | $R_{\text{RMS}}$<br>[nm] |
|---------------------|---------------|----------------|-------------------------------------|------------------------------|--------------------------|
| Untreated samples   |               |                |                                     |                              |                          |
| A                   | ...           | 31             | ...                                 | 197                          | 264±44                   |
| B                   | 780           | 285            | 0.38                                | 1810                         | 333±47                   |
| Pre-treated samples |               |                |                                     |                              |                          |
| A'                  | ...           | 65             | ...                                 | 384                          | 125±38                   |
| B'                  | 800           | 296            | 0.35                                | 1744                         | 145±21                   |

The diamond films were produced using CH<sub>4</sub>/H<sub>2</sub> (1/99 %) gas mixtures. During the deposition the working pressure, the microwave power, the total flow rate and the temperature of the external heater were set constant at 50 mbar, 1000 W, 100 sccm and 700 °C, respectively. Only the process time was varied from 31 to 285 min for the untreated h-BN samples, and from 65 to 296 min for the pre-treated h-BN substrates. Table 1 refers the values of the deposition temperature (T<sub>D</sub>), process time (t<sub>p</sub>), deposition rate (R<sub>D</sub>) and coating thickness (d<sub>coating</sub>) evaluated by in situ pyrometric interferometry (PI), and the root mean square roughness (R<sub>RMS</sub>) of diamond coating determined by atomic force microscopy (AFM).

Prior to plasma deposition, the two samples were submitted to an appropriate ultrasonic pre-treatment in a suspension of 40-60 μm grain size diamond powder for 60 min to promote diamond nucleation on the h-BN surface, thus obtaining the pre-treated samples A' and B'. Differently, the untreated samples A and B were only rinsed, for 5 min each and in sequence, with ethanol, isopropilic alcohol and deionized water, and then dried under N<sub>2</sub> flow. During the plasma chemical process the substrate temperature was kept at approximately 800 °C by both the plasma and the external heater. The surface temperature and the R<sub>D</sub> were monitored for both untreated and pre-treated h-BN sample in-situ and in real-time by the PI technique<sup>32</sup> using a dual wavelength (λ<sub>1</sub>=2.1 and λ<sub>2</sub>=2.4 μm) infrared pyrometer (Williamson Pro 92 40). Precisely, the R<sub>D</sub> is given by the formula:

$$R_D = \frac{(\lambda_1 + \lambda_2) \cdot \cos \theta}{4 \cdot n \cdot \Delta t}$$

where n is the refractive index of the film, θ is the observation angle as measured from the sample surface normal and Δt is the period of the apparent temperature oscillations. The deposition rates (R<sub>D</sub>) were also determined in situ by laser reflectance interferometry (LRI)<sup>33</sup> on pre-treated p-Si for its mirror-like surface.

All samples were characterized by Raman spectroscopy and SEM, AFM microscopies. The chemical–structural features of diamond films were determined at room temperature by means of a Raman confocal micro-spectrometry apparatus (Labram from Jobin-Yvon Horiba) in the backscattering configuration using an Ar-ion laser beam at 488 nm with a laser output power of 4.5 mW. The spot size on the samples was approximately 1 μm diameter by using a 100× dry objective. At least three measurements were acquired from different regions of the samples. The Raman spectra provided a fingerprint for the identification and chemical-structural characterization of diamond films.

The film surface morphology was observed by SEM using a Zeiss EVO 50XV Poperating in the secondary electron mode at a voltage of 15 kV without any use of conductive coating of samples. The morphology of the coatings was also evaluated by AFM using high accuracy poly silicon probe tips characterized by a resonance frequency of 235 kHz and a force constant of 12 N/m. The AFM images were collected in the non-contact mode using a NTEGRA Aura, NT-MDT (Zelenograd, Russia) system operating in air at ambient pressure and room temperature and humidity. The effect of environmental noise was minimised by vibration-resistant housing on a vibration isolation table. Micrographs in the height mode were recorded by sampling the surface at a scan rate of 1.0 Hz with a resolution of 512 x 512 pixels. The AFM images were processed using the Nova software, and average values of the surface root-mean-square roughness (R<sub>RMS</sub>) were estimated on 10 x 10 μm<sup>2</sup> surface areas by sampling five different regions for each film obtained. The AFM provided a very well resolved three-dimensional profile of sample surface, whereas SEM provided a two-dimensional image. In comparison to SEM, AFM in ambient air allowed to obtain an excellent three-dimensional image and provided an optimal analysis of the sample without any treatment (e.g., conductive coating).

### III. RESULTS AND DISCUSSION

As diamond nucleation is difficult to occur on non-diamond substrates, the substrate surface must be pre-treated to promote the primary nucleation density using in situ (bias-enhanced nucleation technique) or ex situ (ultrasonic agitation, seeding and/or deposition of carbon/silicon carbide interlayer) methods. Usually the pre-treatment of non-diamond substrate is necessary to reduce the difference of surface energy between the lattice constants of the substrate and the diamond film to be grown. Without these treatments a very little or no nucleation occurs on most substrates including the silicon substrate. Although the reason for the increased nucleation density is still unknown, it is speculated that the imperfections caused by scratching or energetic particle bombardment are responsible for this effect.<sup>34,35</sup> Lux and Haubner,<sup>36</sup> found that diamond nucleation on c-BN occurred readily. Lately, a feasible heteroepitaxial growth of diamond obtained due to lattice matching between diamond and c-BN substrate or films.<sup>29,30,37</sup> Although a complete and clear picture is not yet available about substrate materials that most favour diamond nucleation, at present no experimental studies report about diamond growth on h-BN

substrates.

Figures 1a-b show the pyrometric interferograms acquired during the diamond growth process on untreated and pre-treated h-BN substrates at short and long process times. The interferograms allow the measurement of deposition onsets and times, and the determination of  $R_D$  and real surface temperature during growth by measuring the oscillation period of the interference fringes,  $\Delta t$ , which is well apparent for long process time ( $>\Delta t$ ) (Fig.1b) and absent for short process time ( $<\Delta t$ ) (Fig.1a), and the average of apparent temperature (horizontal dashed line in Fig. 1b). All related results are reported in Table 1. Further, the difference in the amplitude of interference fringes of PI curves (Fig. 1b) between the untreated B and pre-treated B' samples indicates a different roughness of the growing diamond films on the h-BN surface. The lower is the amplitude, the higher is the roughness. In particular, the  $R_D$  values are quite similar in both B and B' samples. The beginning of PI curves (Figs. 1a and 1b) shows that the deposition process occurs almost-instantaneously, without denoting a nucleation time either in untreated or pre-treated h-BN substrates. Nucleation times usually need from a few minutes to hours,<sup>32,38</sup> depending on the substrate materials, surface pre-treatments and deposition parameters.

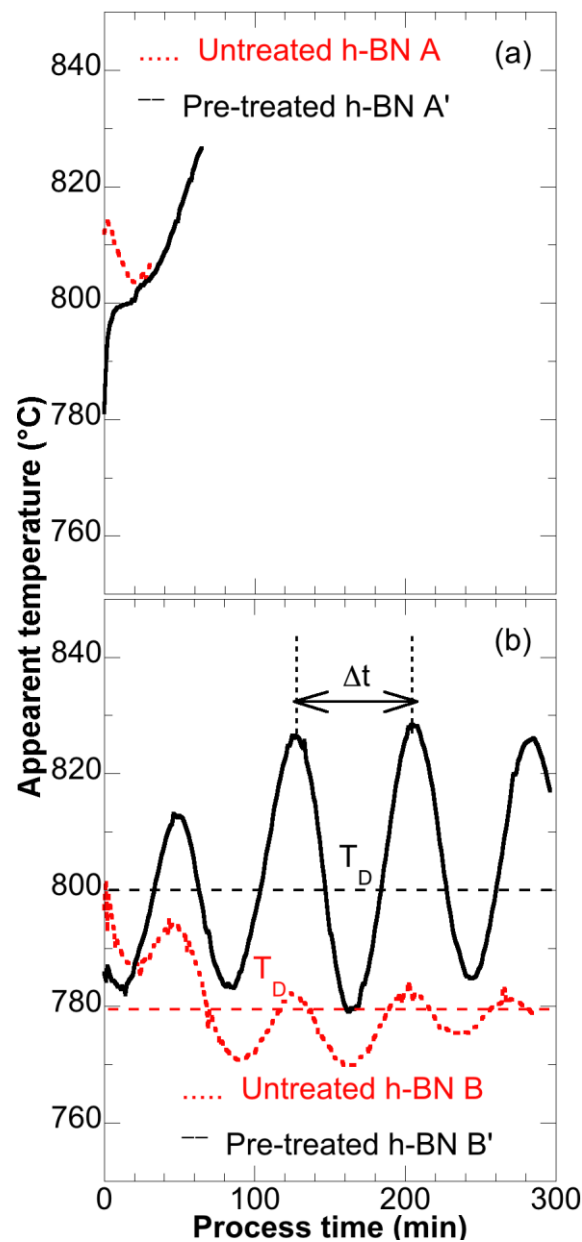


**FIGURE 1. PYROMETRIC INTERFEROGRAMS ACQUIRED DURING THE GROWTH PROCESS ON UNTREATED AND PRE-TREATED H-BN SUBSTRATES AT SHORT (A) AND LONG (B) PROCESS TIMES.**

The Raman spectra of samples (Figs.2a-c) can provide information on the chemical bonding characteristics of the samples.

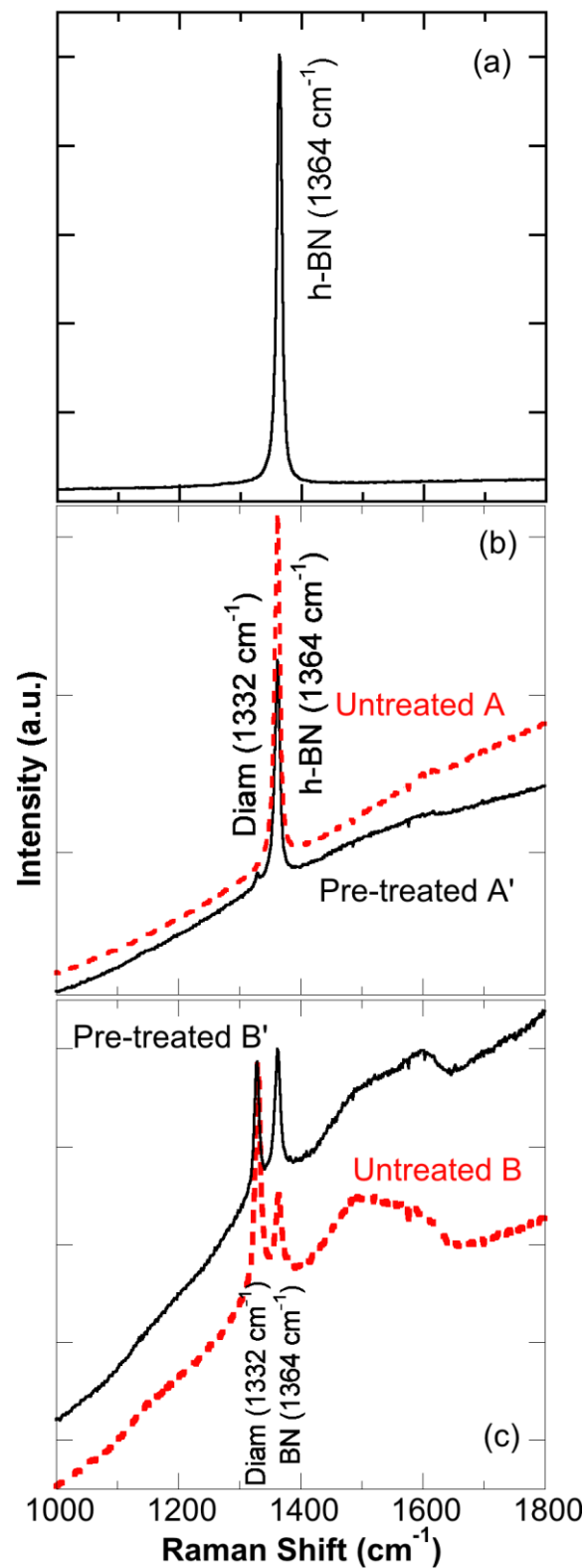
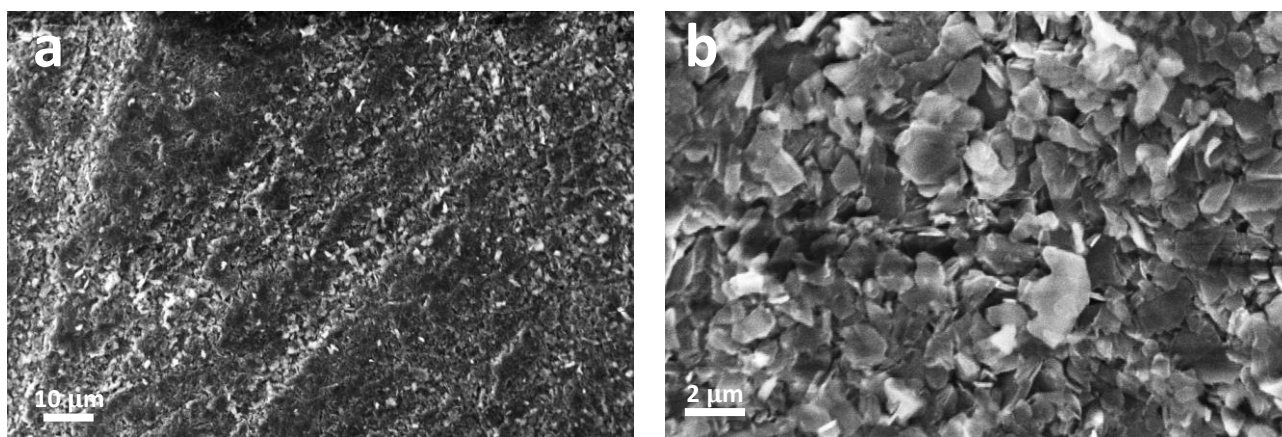


**FIGURE 2. RAMAN SPECTRA OF BULK H-BN SUBSTRATE (A); UNTREATED A AND PRE-TREATED A' SAMPLES AT SHORT PROCESS TIME (B); UNTREATED B AND PRE-TREATED B' SAMPLES AT LONG PROCESS TIME (C).**

The Raman-active phonon of the bulk h-BN substrate is centred at  $1364\text{ cm}^{-1}$  [39] (Fig. 2a). The spectrum of the untreated, 197-nm-thick (due to the short deposition time) sample A (Figure 2b) features: (i) a main peak of the bulk h-BN centred at around  $1364\text{ cm}^{-1}$ ; (ii) a strong fluorescence background due to structural defects and impurities of the very thin diamond layer; and (iii) a weak broad band centred at about  $1600\text{ cm}^{-1}$ , attributed to graphitic and disordered  $\text{sp}^2$  components localized at grain boundaries.<sup>40,41</sup> The Raman spectrum of the pre-treated, 384-nm-thick sample A' (Fig. 2b) is very similar to that of the untreated sample A, but shows also a very weak diamond peak at  $1332\text{ cm}^{-1}$ . The spectra of 1810-nm and 1744-nm-thick samples B and B' (Fig. 2c) show a high contribution of the diamond peak at  $1332\text{ cm}^{-1}$ , which appears of equal or even higher intensity than the h-BN peak at  $1364\text{ cm}^{-1}$ , and an intense broad band of  $\text{sp}^2$  carbon at about  $1550\text{-}1600\text{ cm}^{-1}$ . The intensity of both signals increases with increasing the thickness of diamond coatings (see Table 1).

Figures 3a and 3b show the SEM images of the surface of the bulk untreated h-BN substrate at lower and higher magnification, respectively. A non-smooth surface made mainly by striations and furrows is visible clearly in Figure 3a, where as a plate-like particle structure is evident in Figure 3b.

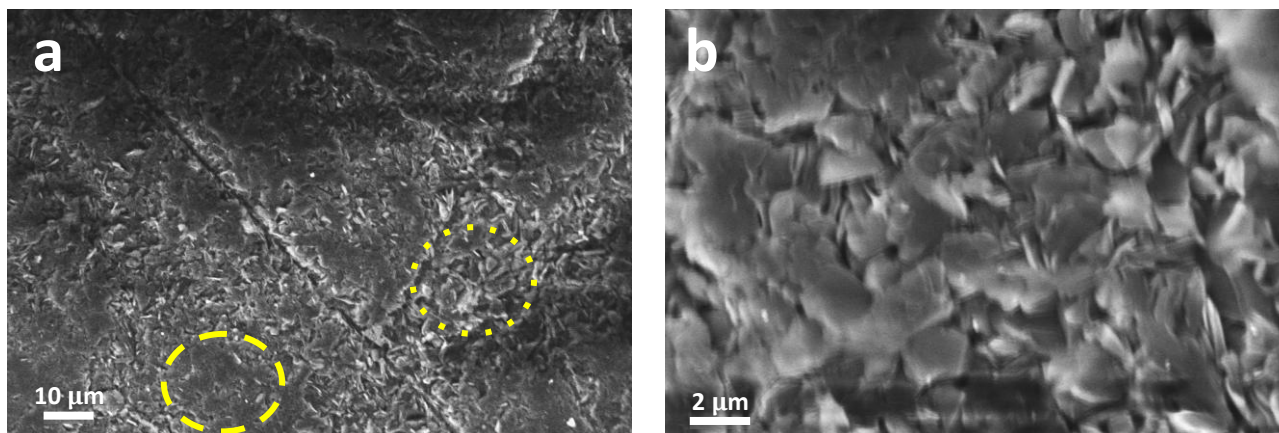
#### Untreated sample A (197 nm thickness)



**FIGURE 3. SEM IMAGES AT DIFFERENT MAGNIFICATIONS (A,B) OF THE BULK H-BN SUBSTRATE.**

Figures 4a-b and 4c-d show the SEM images at different magnifications of untreated sample A (197-nm-thick) and pre-treated sample A' (384-nm-thick). The very thin coverage of untreated sample A still provides evidence of plate-like particles (Figs. 4a-b), where as diamond grains barely appear. The yellow dashed circle in Fig. 4a shows an area that appear barely smooth due to the diamond coating, whereas the yellow dotted circle shows a bulk h-BN substrate with plate-like surface. On the other hand the pre-treated sample A' (384-nm-thick) exhibits sub-microcrystals that cover almost continuously the substrate surface (Figs. 4c-d). The red dashed circles in Figures 4c-d are focused on restricted regions where plate-like particles are still evident in the background.

#### Pre-treated sample A' (384 nm thickness)



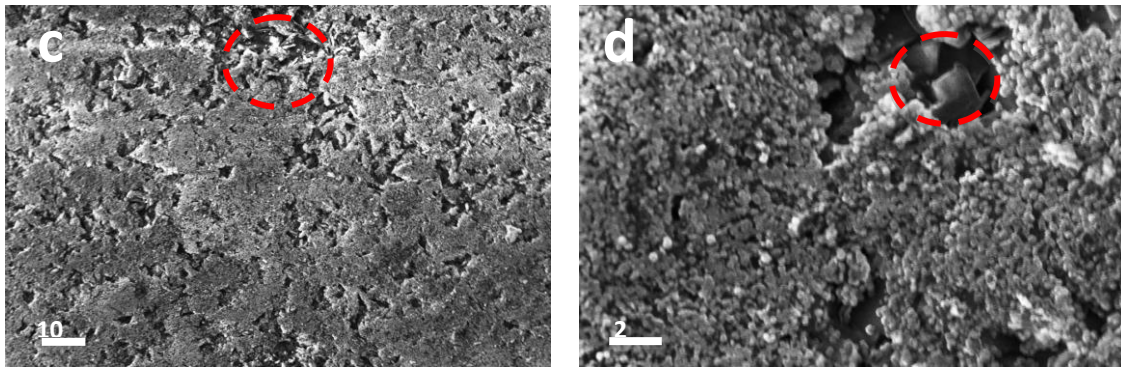


**FIGURE 4. SEM IMAGES AT DIFFERENT MAGNIFICATIONS OF THE 197-NM-THICK UNTREATED SAMPLE A (A, B), AND THE 384-NM-THICK PRE-TREATED SAMPLE A' (C, D). THE YELLOW DASHED CIRCLE IN (A) SHOWS AN AREA THAT APPEAR BARELY SMOOTH DUE TO THE DIAMOND COATING, WHEREAS THE YELLOW DOTTED CIRCLE SHOWS A BULK H-BN SUBSTRATE WITH PLATE-LIKE SURFACE. THE RED DASHED CIRCLES IN (C) AND (D) SHOW RESTRICTED REGIONS WHERE A PLATE-LIKE SURFACE IS STILL EVIDENT.**

Figures 5a-d show the SEM images at different magnifications of the 1810-nm-thick untreated sample B and 1744-nm-thick pre-treated sample B'. The untreated sample B at the deposition time of 296 min features faceting and coalescence of individual crystallites with an average diameter of 2  $\mu\text{m}$  (Figs. 5a-b). In particular, Figure 5a shows the h-BN substrate completely covered by diamond crystals grown on the initially rough substrate, thus they appear to be placed at different heights, so providing the effect of a non-homogeneous surface. As a result, the h-BN plate-like particles appear completely covered by some well-formed, pyramidal-shaped diamond crystallites. On the other hand (Figs. 5c-d) show that on pre-treated sample B' after long time process (285 min, deposition time) the crystals grow homogeneously in size and faceting on the h-BN substrate in almost the same plane.

#### Untreated sample B(1810 nm thickness)

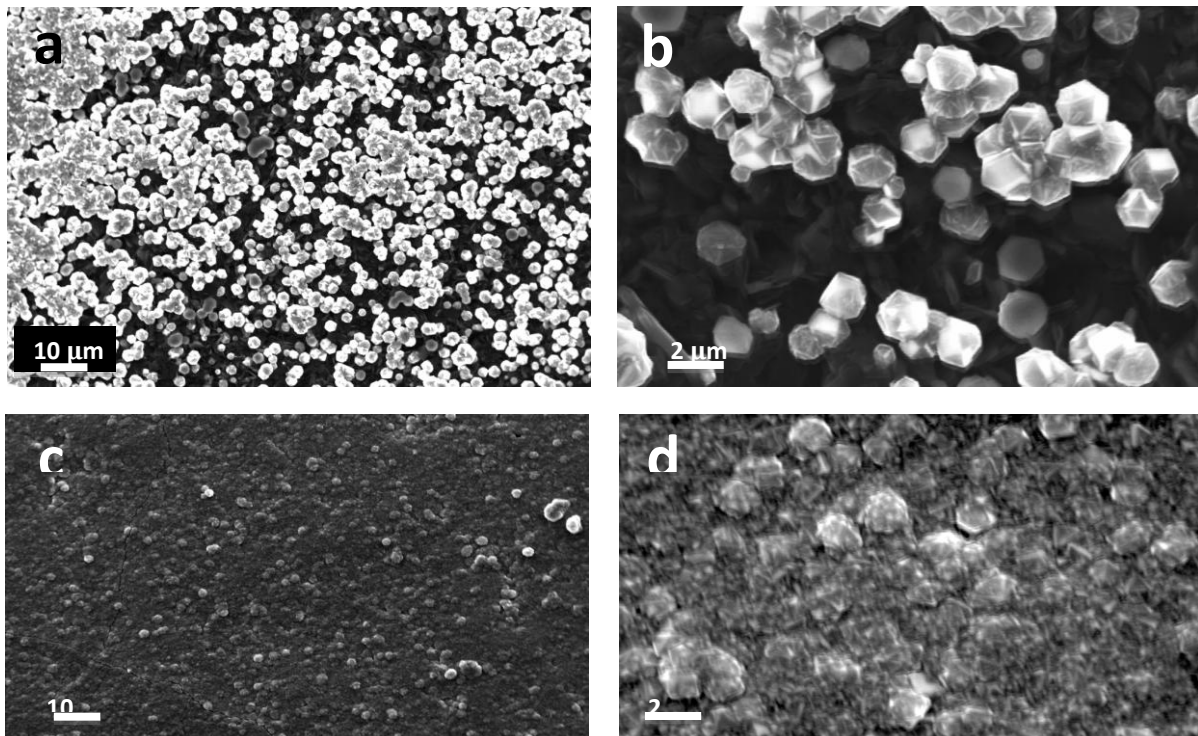
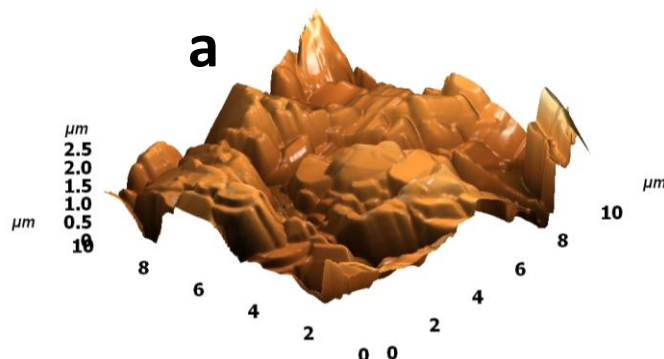


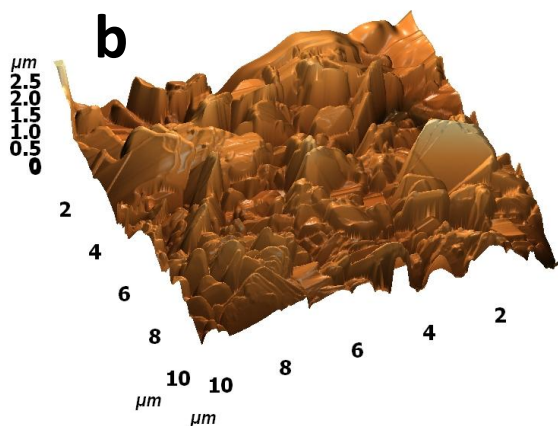
**FIGURE 5. SEM IMAGES OF THE 1810-NM-THICK UNTREATED SAMPLE B (A, B) AND 1744-NM-THICK PRE-TREATED SAMPLE B' (C, D).**

The 3D AFM images supported by previous SEM images clearly show several distinguishable topographical growth stages of diamond coatings on the surface of bulk h-BN (Figs. 6a-e).

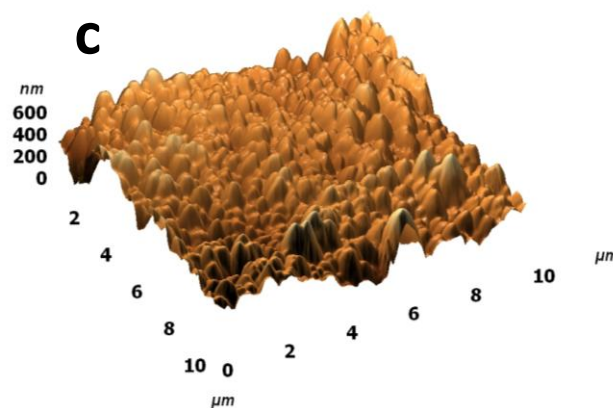
**Bulk h-BN substrate**



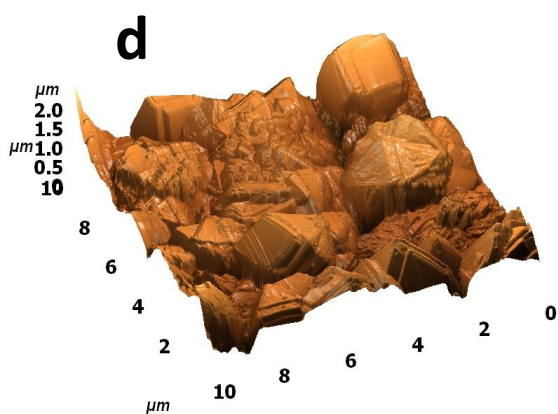
**Untreated sample A (197 nm thick)**



**Pre-treated sample A' (384 nm thick)**



**Untreated sample B (1810 nm thick)**



**Pre-treated sample B' (1744 nm thick)**

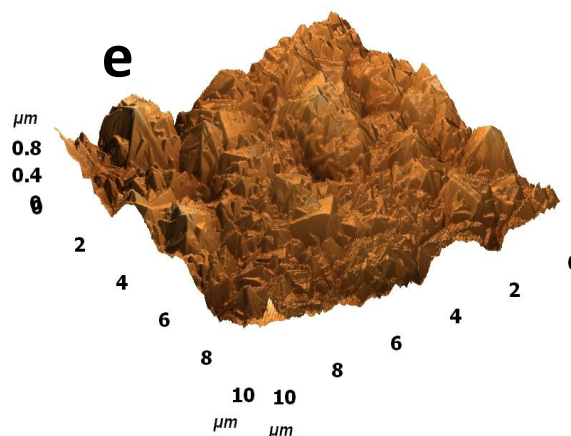


**FIGURE 6.3D TOPOGRAPHY AFM IMAGES (10X10 μM<sup>2</sup>) OF THE BULK H-BN SUBSTRATE (A), UNTREATED AND PRE-TREATED SAMPLES A AND A' (B AND C), AND UNTREATED AND PRE-TREATED SAMPLES B AND B' (D AND E).**

Due to the different morphology of the samples, the  $R_{\text{RMS}}$  values reported in Table 1 and calculated by AFM show an unexpected trend, i.e. the  $R_{\text{RMS}}$  values do not grow increasing the coating thickness ( $d_{\text{coating}}$ ). In particular, after short process times (31 and 65 min) the h-BN  $R_{\text{RMS}}$  value of 397 nm decreases to  $264 \pm 44$  nm and  $125 \pm 38$  nm, respectively, for the untreated and pre-treated samples. The reduced  $R_{\text{RMS}}$  values confirm the marked difference in topography (Figs. 6b-c) between the untreated and the pre-treated samples. This behaviour is probably due to the ultrasonic pre-treatment effect that is inducing a soft smoothing of the h-BN substrate. This topographical difference (Figs. 6d-e) persists also at high coating thickness, when the process time increases to 285 min for the untreated sample B and to 296 min for the pre-treated sample B'. In particular, the surface appears quite smooth, with an  $R_{\text{RMS}}$  value of  $145 \pm 21$  nm, for the pre-treated sample B', whereas the  $R_{\text{RMS}}$  value for the untreated sample B increases up to  $333 \pm 47$  nm due to the size increase of large crystals on the substrate. Often these crystallites exhibit a pseudo five-fold symmetry (Fig. 6d) due to multiple twinning. The lattice strains present in multiply twinned sub-micro-particles (Figs. 7 a-b) can be easily accommodated due to their small dimensions, and often one or more of the twinned regions show lattice spacings that are altered slightly. Multiply twinned nanoparticles growth has been observed also on the c-BN crystals at shorter deposition time (40 min).<sup>42</sup>

Similar  $R_{\text{RMS}}$  values are obtained at the different coating thickness for pre-treated samples at short and long times. The untreated h-BN samples at short and long times also show a diamond coating growth that reaches almost the same thickness, but with higher values of  $R_{\text{RMS}}$ , with respect to the pre-treated h-BN samples. This experimental evidence found is in contrast with theoretical results calculated by Johansson et al.,<sup>17</sup> who revealed a small probability of diamond nucleation on untreated h-BN.

The diamond coating growth on untreated h-BN samples may be ascribed mainly to the high  $R_{\text{RMS}}$  values of the initial substrate, which promotes quickly the nucleation and growth of diamond following the original sample topography so acting as a memory effect. In particular, the high  $R_{\text{RMS}}$  value of the bulk h-BN appears also to be transferred to the growth at long time process of crystallites with an average diameter of 2  $\mu\text{m}$  and a pseudo five-fold symmetry.

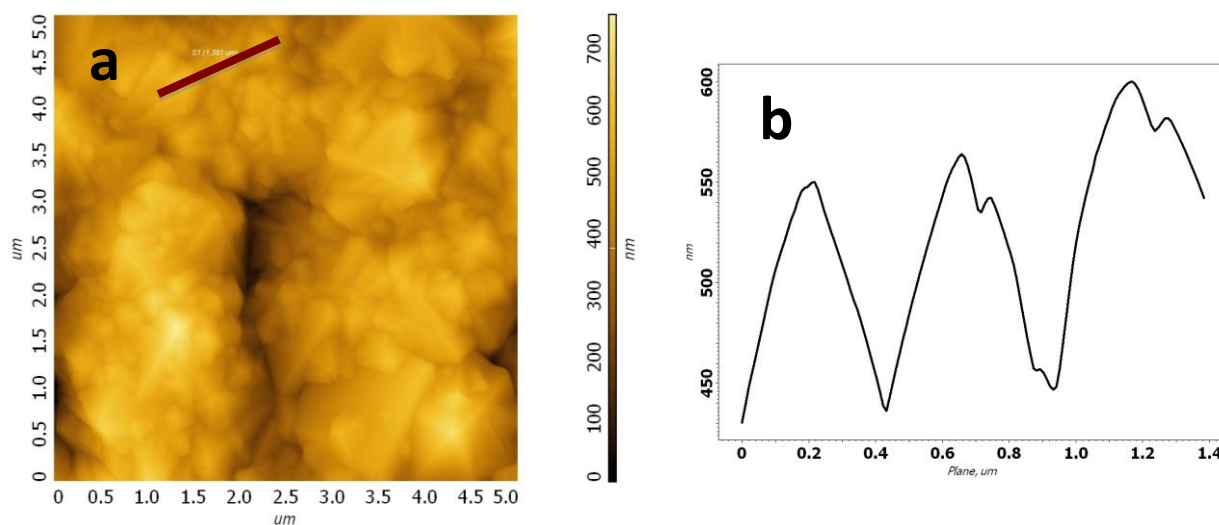


**FIGURE 7. 2D TOPOGRAPHY AFM IMAGE OF THE PRE-TREATED SAMPLE B' (A) AND ITS PROFILE SCANNED ALONG THE RED LINE, THE SECOND AND THIRD PEAK FROM THE RIGHT SHOW TWINNED CRYSTALS (B).**

#### IV. CONCLUSION

This work for the first time investigated comparatively untreated and pre-treated h-BN substrates, and studied the influence of substrate nature on the morphology of diamond coatings synthesized by MWPECVD.

The diamond coating growth on untreated h-BN samples has shown an unexpected higher  $R_{\text{RMS}}$  value compared to the pre-treated h-BN samples as measured by AFM and confirmed by the lower amplitude of interference fringes of PI curve. This behaviour was due to the initial rough topography of the h-BN substrate. A number of diamond crystals with peculiar shapes and showing a five-fold symmetry due to multiple twinning were observed by SEM and AFM. These materials appear promising for use as protecting coatings of surfaces against erosion when in contact with particles of various size range and/or by high velocity fluid impingement.

### ACKNOWLEDGEMENTS

This study was carried out within the framework of the Project PON03PE\_00067\_6 “APULIA SPACE”, (Italy). The authors are grateful to Prof. R. Laviano of University of Bari, Dipartimento di Scienze della Terra e Geoambientali, Italy for the use of the SEM, Prof. G. Carbone of Politecnico di Bari, Italy for the use of the AFM, Dr. G. Perna and Prof. V. Capozzi of University of Foggia, Dipartimento di Scienze Biomediche for Raman spectroscopy measurements and Alta SPA for providing the h-BN samples.

### REFERENCES

- [1] J. T. Yim, M.L. Falk and I.D. Boyd: “Modeling low energy sputtering of hexagonal boron nitride by xenon ions”, *J. Appl. Phys.*, 2008, 104, 123507.
- [2] Y. K. Yap, J. Menda, L. K. Vanga, V. Kayastha, J. Wang, L. B. King, S. Dimovski and Y. Gogotsi: “Testing Multiwall Carbon Nanotubes on Ion Erosion for Advanced Space Propulsion”, *Mat. Res. Soc. Symp. Proc.*, 2004, 821, P3.7.1.
- [3] T. Haag, M. Patterson, V. Rawlin and G. Soulas: “Carbon-based optics development at NASA GRC”, *Proc. 27th Int. Electric Propulsion Conf.*, October 2001. Paper IEPC-01-94.
- [4] J. J. Blandino, D. G. Goodwin and C.E. Garner: “Low energy sputter yields for diamond, carbon-carbon composite, and molybdenum subject to xenon ion bombardment”, *Diamond & Relat. Mater.*, 2000, 9, 1992-2001.
- [5] A. Lipp, K. A. Schwetz and K. Hunold: “Hexagonal Boron Nitride: fabrication, properties, and applications”, *J. Eur. Ceram. Soc.*, 1989, 5, 3-9.
- [6] L. Vel, G. Demazeau and J. Etourneau: “Cubic boron nitride: synthesis, physicochemical properties and applications”, *Mater. Sci. Eng.*, 1991, 10, 149-164.
- [7] P. B. Mirkarimi, K. F. McCarty and D.L. Medlin, “Review of advances in cubic boron nitride film synthesis”, *Mater. Sci. Eng., R.*, 1997, 21, 47-100.
- [8] M. Britton, D. Waters, R. Messer, E. Sechkar and B. Banks: “Sputtering erosion measurement on boron nitride as a Hall thruster material”, *NASA/TM*, 2002, 211837.
- [9] K. S. Lee, Y. S. Kim, M. Tosa, A. Kasahara and K. Yosihara: “Mechanical properties of hexagonal boron nitride synthesized from film of Cu/BN mixture by surface segregation”, *App. Surf. Sci.*, 2001a, 169-170, 420-424.
- [10] K. S. Lee, Y. S. Kim, M. Tosa, A. Kasahara and K. Yosihara: “Hexagonal boron nitride film substrate for fabrication of nanostructures”, *App. Surf. Sci.*, 2001b, 169-170, 415-419.
- [11] Y. S. Kim, K. S. Lee, J. Lee, M. Tosa, A. Kasahara and K. Yosihara: “Surface segregation of hexagonal boron nitride and its surface properties”, *J. Vac. Sci. Technol. A*, 2001, 19, 1013-1017.
- [12] M. Corso, W. Auwärter, M. Muntwiler, A. Tamai, T. Greber and J. Osterwalder: “Boron Nitride Nanomesh”, *Science* 2004, 303, 217-220.
- [13] M. Corso, T. Greber and J. Osterwalder: “h-BN on Pd(110): a tunable system for self-assembled nanostructures?”, *Surf. Sci.*, 2005, 577, L78-L84.
- [14] J. Olander, M. Ottosson, P. Heszler, J. O. Carlsson and K. Larsson: “Laser-assisted atomic layer deposition of boron nitride thin films”, *Chem. Vap. Deposition* 2005, 11, 330-337.
- [15] T. Greber, L. Brandenberger, M. Corso, A. Tamai and J. Osterwalder: “Single layer hexagonal boron nitride films on Ni(110)”, *e-J. Surf. Sci. Nanotech.*, 2006, 4, 410-413.
- [16] M. Morscher, M. Corso, T. Greber and J. Osterwalder: “Formation of single layer h-BN on Pd (111)”, *Surf. Sci.*, 2006, 600, 3280-3284.
- [17] E. Johansson, K. Larsson and J. O. Carlsson: “Diamond nucleation on hexagonal boron nitride: An ab initio study of energetics”, *J. Phys. Chem.*, 1995, 99, 12781-12785.
- [18] M. Carbone, K. Larsson and J. O. Carlsson: “Diamond nucleation on hexagonal boron nitride: A theoretical investigation of the influence of nearest substituents”, *J. Phys. Chem. A*, 1997, 101, 9445-9448.
- [19] M. Carbone, K. Larsson and J. O. Carlsson: “Diamond nucleation on hexagonal boron nitride: A theoretical investigation of the influence of CH<sub>3</sub> and Na substituents”, *J. Phys. Chem. B*, 1998, 102, 5866-5869.
- [20] B. Mårlid, K. Larsson and J. O. Carlsson: “Hydrogen and fluorine adsorption on the h-BN plane”, *J. Phys. Chem. B*, 1999, 103, 7637-7642.
- [21] B. Mårlid, K. Larsson and J. O. Carlsson: “Nucleation of c-BN on hexagonal boron nitride”, *Phys. Rev. B*, 2001, 64, 184107.
- [22] J. Olander and K. Larsson: “Initial growth of hexagonal and cubic boron nitride: A theoretical study”, *Phys. Rev. B*, 2003, 68, 075411.
- [23] X. Ding, G. Ding, X. Xie, F. Huang and M. Jiang, “Direct growth of few layer graphene on hexagonal boron nitride by chemical vapor deposition”, *Carbon* 2011, 49, 2522-2525.
- [24] Y. Kimura, T. Wakabayashi, K. Okada, T. Wada and H. Nishikawa: “Boron nitride as a lubricant additive”, *Wear* 1999, 232, 199-206.
- [25] P. Tequi, B. Constans, S. Iovine, R. Ladaviere, J. M. Martin and M.T. Le: “Additive composition for transmission oil containing hydrated alkali metal borate and hexagonal boron nitride”, *Eur. Pat. Appl.* 2004, EP 1386956.
- [26] P. Tequi, B. Constans, S. Iovine and R. Ladaviere: “Additive composition for transmission oil containing hexagonal boron nitride and viscosity index improver”, *Eur. Pat. Appl.* 2005, EP 1535987.
- [27] F. K. Botz and M.A. Handley: “Film-forming metal working lubricating oil containing glyceridic oils and hexagonal boron nitride”, *PCT Int. Appl. WO* 2005, 108530.

- [28] N. B.Meezan, N.Gasconand M.A. Cappelli: "Linear geometry hall thruster with boron nitride and diamond walls", Proc.27th Int. Electric Propulsion Conf. October 2001. Paper IEPC-01-039.
- [29] S.Koizumi and T.Inuzuka:"Initial growth process of epitaxial diamond thin films on cBN single crystals",Jpn. J. Appl. Phys.,1993, 32, 3920– 3927.
- [30] W.P. Chai, Y. S.Gu, M. Li, Z. H. Mai, Q. Z. Li, L. Yuanand S.J. Pang:"Epitaxial growth of diamond films on the {221} and {100} surfaces of cBN with microstructures full of (100) facets",Appl. Phys. Lett.,1994, 64, 1941.
- [31] M. C. Polo, G. Sanchez, W. L. Wang, J.Esteveand J.L. Andujar:"Growth of diamond films on boron nitride thin films by bias-assisted hot filament chemical vapor deposition",Appl. Phys. Lett., 1997,70, 1682-1684.
- [32] G. Cicala, R. Brescia, M.A. Nitti, A. Romeo, D. Altamura, C. Giannini, M. Capitelli, P.Spinelliand S. Schutzmann:"Study of polycrystalline diamond deposition by continuous and pulsed discharges",Surf. Coat. Technol.,2010,204, 1884–1888.
- [33] G. Cicala, V.Magaletti, G. S.Senesiand M.Tamborra:"Smoothness improvement of micrometerandsubmicrometer-thick nanocrystalline diamond films produced by MWPECVD", J. Nanopart. Res.,2013, 15, 1549.
- [34] Z. P. Lu, J.Heberleinand E. Pfender, "Process study of thermal plasma Chemical Vapor Deposition of diamond, part II: Pressure dependence and effect of substrate pretreatment",Plasma Chem.& Plasma Proc.,1992, 12, 55-69.
- [35] Y.Lifshitz, X. M.Meng, S. T. Lee, R.AkhveldianyandA. Hoffman:"Visualization of diamond nucleation and growth from energetic species",Phys. Rev. Lett.,2004, 93, 056101.
- [36] B. Lux and R.Haubner:"Nucleation and growth of low-pressure diamond", in "Diamond and Diamond-like Films and Coatings", (ed. E. Clausinget al.), 579-609; 1991, New York, Plenum Press.
- [37] T. A.Friedmann, L. J.Bernardez, K. F. McCarty, E. J. Klaus, D. K.Ottesen, H.A.Johnsenand W.M. Clift:"Diamond deposition on polycrystalline films of cubic boron nitride",Appl. Phys. Lett., 1993,63, 1342-1344.
- [38] R. A.Bauer, N. M.Sbrockey and W. E.Brower, Jr:"Quantitative nucleation and growth studies of PACVD diamond film formation on (100) silicon",J. Mater. Res.,1993,8, 2858-2869.
- [39] S. Reich, A. C. Ferrari, R.Arenal, A.Loiseau, I. Belloand J. Robertson: "Resonant Raman scattering in cubic and hexagonal boron nitride",Phys. Rev. B,2005, 71, 205201.
- [40] A. C. Ferrari andJ.Robertson: "Origin of the 1,150 cm<sup>-1</sup> Raman mode in nanocrystalline diamond",Phys. Rev. B,2001, 63, 121405.
- [41] R. Pfeiffer, H. Kuzmany, P. Knoll, S.Bokova, N. Salkand B. Gunther:"Evidence for trans-polyacetylene in nanocrystalline diamond films",Diam. Relat. Mater.,2003, 12, 268–271.
- [42] L. Nistor, V.Buschmann, V.Ralchenko, G. Dinca, I.Vlasov, J. Van Landuytand H. Fuess: "Microstructural characterization of diamond films deposited on c-BN crystals",Diamond &Relat. Mater.,2000, 9, 269-273.